Synthesis of Bulk and Alumina-Supported Bimetallic Carbide and Nitride Catalysts

Scott Korlann, Brian Diaz, and Mark E. Bussell*

Department of Chemistry, MS-9150, Western Washington University, Bellingham, Washington 98225

Received October 19, 2001. Revised Manuscript Received July 26, 2002

A new synthesis for the preparation of the bimetallic carbide, Co_3Mo_3C, as well as syntheses for the preparation of alumina-supported Ni_2Mo_3N, Co_3Mo_3N, and Co_3Mo_3C are described. The syntheses utilize the temperature-programmed reduction (TPR) method in which solid-state precursors are converted to the desired products in the presence of gas-phase reactants. Bulk and alumina-supported Co_3Mo_3C is prepared in a two-step synthesis in which oxide precursors are converted to Co_3Mo_3N, which is subsequently carburized to give the bimetallic carbide. Alumina-supported Ni_2Mo_3N and Co_3Mo_3N are prepared from supported oxide precursors via nitridation in flowing NH_3, while the carburization of bulk and alumina-supported Co_3Mo_3N utilizes a CH_4/H_2 mixture to yield the bimetallic carbide products. Elemental analysis of a 22.5 wt % Co_3Mo_3C/Al_2O_3 catalyst suggests incomplete replacement of N with C under the synthesis conditions employed. The alumina-supported carbide and nitride materials have high surface areas and O_2 chemisorption capacities, suggesting that these syntheses provide an excellent route for the preparation of heterogeneous catalysts in which bimetallic carbides and nitrides are the active component.

Introduction

Monometallic and bimetallic carbides and nitrides of early transition metals have drawn considerable interest in recent years for their potential use as heterogeneous catalysts in a variety of industrial processes.[1,2] To be useful as heterogeneous catalysts, the carbide and nitride materials must possess high surface areas, and the temperature-programmed reduction (TPR) synthesis method has been shown to be particularly successful in this regard. Unsupported carbide and nitride catalysts typically have surface areas in the range 30−100 m^2/g,[3,4] while oxide-supported materials can have surface areas well over 100 m^2/g and high dispersion of the carbide or nitride phase.[5−7]

Hydrotreating, in which S, N, and O impurities are removed from fossil fuel feedstocks, is an area of catalysis in which early transition metal carbides and nitrides have attracted significant interest. Industrial hydrotreating catalysts typically consist of alumina-supported molybdenum promoted with either cobalt or nickel and the catalysts are sulfided prior to use.[8] Studies in a number of laboratories over the past few years have shown alumina-supported molybdenum carbide (β-Mo_2C)[5,6,9] and nitride ((γ-Mo_2N)[6,9−12] to be more active hydrodesulfurization (HDS) catalysts than conventional sulfided molybdenum catalysts. More recently, a number of laboratories have investigated the hydrotreating properties of unsupported Co_3Mo_3N[13,14] and Co−Mo−C phases[15,16] as well as supported nitrided materials containing Mo with either Co or Ni.[17−23] In

* To whom correspondence should be addressed. Prof. Mark E. Bussell, Department of Chemistry, MS-9150, Western Washington University, 516 High St., Bellingham, WA 98225-9150. Tel.: 360-650-3145. Fax: 360-650-2826. E-mail: Mark.Bussell@wwu.edu.

(1) Oyama, S. T. *Catal. Today* **1992**, *15*, 172.
(2) Oyama, S. T. Introduction to the Chemistry of Transition Metal Carbides and Nitrides. In *The Chemistry of Transition Metal Carbide and Nitrides*; Oyama, S. T., Ed.; Blackie Academic & Professional: New York, 1996; p 1.
(3) Ramanathan, S.; Oyama, S. T. *J. Phys. Chem.* **1995**, *99*, 16365.
(4) Claridge, J. B.; York, A. P. E.; Brungs, A. J.; Green, M. L. H. *Chem. Mater.* **2000**, *12*, 132.
(5) Sajkowski, D. J.; Oyama, S. T. *Appl. Catal. A* **1996**, *134*, 339.
(6) McCrea, K. R.; Logan, J. W.; Tarbuck, T. L.; Heiser, J. L.; Bussell, M. E. *J. Catal.* **1997**, *171*, 255.
(7) Miyao, T.; Shishikura, I.; Matsuoka, M.; Nagai, M.; Oyama, S. T. *Appl. Catal. A* **1997**, *165*, 419.
(8) Topsøe, H.; Clausen, B.; Massoth, F. E. Hydrotreating Catalysis. In *Catalysis*: *Science and Technology*; Anderson, J. R., Boudart, M., Eds.; Vol. 11; Springer-Verlag: Berlin, 1996; p 1.
(9) Aegerter, P. A.; Quigley, W. W. C.; Simpson, G. J.; Ziegler, D. D.; Logan, J. W.; McCrea, K. R.; Glazier, S.; Bussell, M. E. *J. Catal.* **1996**, *164*, 109.
(10) Nagai, M.; Miyao, T.; Tuboi, T. *Catal. Lett.* **1993**, *18*, 9.
(11) Nagai, M.; Uchino, O.; Kusgaya, T.; Omi, S. In *Hydrotreatment and Hydrocracking of Oil Fractions*; Froment, G., Delmon, B., Grange, P., Eds.; Elsevier: New York, 1997; p 541.
(12) Nagai, M.; Kiyoshi, M.; Tominaga, H.; Omi, S. *Chem. Lett.* **2000**, 702.
(13) Kim, D.-W.; Lee, D.-K.; Ihm, S.-K. *Catal. Lett.* **1997**, *43*, 91.
(14) Ihm, S.-K.; Kim, D.-W.; Lee, D.-K. Effects of Sulfidation of Mo Nitride and CoMo Nitride Catalysts. In *Studies in Surface Science and Catalysis*; Bartholomew, C. H., Fuentes, G. A., Eds.; Elsevier Science: New York, 1997; Vol. 111; p 343.
(15) Xiao, T.-C.; York, A. P. E.; Al-Megren, H.; Claridge, J. B.; Wang, H.-T.; Green, M. L. H. *C. R. Acad. Sci. Paris, Ser. IIc* **2000**, *3*, 451.
(16) Xiao, T.-C.; York, A. P. E.; Al-Megren, H.; Williams, C. V.; Wang, H.-T.; Green, M. L. H. *J. Catal.* **2001**, *202*, 100.
(17) Park, H. K.; Lee, J. K.; Yoo, J. K.; Ko, E. S.; Kim, D. S.; Kim, K. L. *Appl. Catal. A* **1997**, *150*, 21.
(18) Yang, S.; Jiang, X.; Yan, W.; Ying, P.; Xin, Q. *Chin. J. Catal.* **1997**, *18*, 179.
(19) Logan, J. W.; Heiser, J. L.; McCrea, K. R.; Gates, B. D.; Bussell, M. E. *Catal. Lett.* **1998**, *56*, 165.
(20) Chu, Y.; Wei, Z.; Yang, S.; Li, C.; Xin, Q.; Min, E. *Appl. Catal. A* **1999**, *176*, 17.
(21) Miga, K.; Stanczyk, K.; Sayag, C.; Brodzki, D.; Djega-Mariadassou, G. *J. Catal.* **1999**, *193*, 63.
(22) Trawczynski, J. *Appl. Catal. A* **2000**, *197*, 289.

10.1021/cm011508j CCC: $22.00
Published on Web 09/06/2002

the cases of the supported catalysts, the nitrides were impure and it is not possible to ascribe the catalytic properties to a single phase.

In the current study, we report a new synthesis for the preparation of the bimetallic carbide, Co_3Mo_3C, as well as syntheses for the preparation of alumina-supported Ni_2Mo_3N, Co_3Mo_3N, and Co_3Mo_3C.

Experimental Methods

Catalyst Synthesis. *Synthesis of Ni_2Mo_3N and Ni_2Mo_3N/Al_2O_3.* An oxide precursor to Ni_2Mo_3N was prepared by dissolving a mixture of nickel nitrate ($(Ni(NO_3)_2 \cdot 6H_2O$, Alfa Aesar, 99.9985%) (5.165 g, 17.76 mmol) and ammonium heptamolybdate ($(NH_4)_6Mo_7O_{24} \cdot 4H_2O$, Fisher, A.C.S. grade) (4.705 g, 3.807 mmol) in 120 mL of deionized water, evaporating to dryness, and calcining at 773 K for 2 h in air. A light green powder was obtained after calcination. The oxide precursor was converted to Ni_2Mo_3N using temperature-programmed reduction (TPR) in flowing ammonia; the synthesis apparatus has been described in detail elsewhere.[9] Approximately 0.5 g of the oxide precursor was placed onto a quartz wool plug located in a quartz U-tube which was then placed in a tubular furnace. The sample was degassed for 30 min at 295 K followed by 1 h at 393 K, both in 60 sccm He (Airgas, 99.999%). The He was purified prior to use by passing it through 5A molecular sieve (Alltech) and O_2 (Oxyclear) purification traps. Following degassing, the sample was heated from 393 to 1173 K at a rate of 5 K/min in 30 sccm ammonia (NH_3, Airgas, 99.99%) and the sample was then furnace-cooled to room temperature in the ammonia flow. The ammonia was purified in the same manner as was described above for the He. Following furnace cooling, the Ni_2Mo_3N product was passivated for 3 h in a 60 sccm flow of 1 mol % O_2/He (Airgas) prior to air exposure.

Alumina-supported oxide precursors to Ni_2Mo_3N/Al_2O_3 catalysts with theoretical loadings of 10, 15, 20, 25, 30, and 50 wt % Ni_2Mo_3N were prepared by impregnation of finely ground alumina (γ-Al_2O_3, Engelhard Al-3945, 1/12 in. extrusions) with aqueous solutions of $Ni(NO_3)_2 \cdot 6H_2O$ and $(NH_4)_6Mo_7O_{24} \cdot 4H_2O$ followed by calcination in air. For example, the precursor to the 30 wt % Ni_2Mo_3N/Al_2O_3 catalyst was prepared by impregnation of γ-Al_2O_3 (11.08 g) with an aqueous solution of $(NH_4)_6Mo_7O_{24} \cdot 4H_2O$, resulting in 6.00 g of $(NH_4)_6Mo_7O_{24}$ on the support after drying at 393 K and subsequent impregnation with an aqueous solution of $Ni(NO_3)_2 \cdot 6H_2O$ to give 6.59 g $Ni(NO_3)_2$ on the support after drying. The impregnated alumina was calcined and then nitrided as described above to give a 30 wt % Ni_2Mo_3N/Al_2O_3 catalyst. The Ni_2Mo_3N/Al_2O_3 catalysts with the other Ni_2Mo_3N loadings were prepared similarly.

Synthesis of Co_3Mo_3N and Co_3Mo_3N/Al_2O_3. An oxide precursor to Co_3Mo_3N was prepared by dissolving cobalt chloride ($(Co(Cl)_2 \cdot 6H_2O$, Alfa Aesar, 99.9%) (5.0436 g, 21.198 mmol) in approximately 30 mL of deionized water. This solution was added dropwise over 20 min with stirring to a second solution consisting of sodium molybdate, ($Na_2MoO_4 \cdot 2H_2O$, Fisher, A.C.S. grade) (5.1288 g, 21.198 mmol) dissolved in 40 mL of deionized water. The purple precipitate was collected, rinsed with chilled deionized water, chilled ethanol, and a final rinse with chilled deionized water. The sample was dried overnight at 393 K and then calcined at 773 K for 2 h in air. Following grinding to a fine powder, the oxide precursor was recalcined at 773 K for 2 h in air. The oxide precursor was converted to Co_3Mo_3N via TPR in flowing ammonia using the system described briefly above and in detail elsewhere.[9] Approximately 0.5 g of the oxide precursor was degassed for 1 h at 295 K in 60 sccm He. Following degassing, the sample was heated from 295 to 1023 K at a rate of 0.5 K/min in 100 sccm NH_3 and held at 1023 K in the ammonia flow for 12 h. The Co_3Mo_3N product was furnace-cooled to room temperature in flowing ammonia and then passivated in a 60 sccm flow of 1 mol % O_2/He for 3 h prior to air exposure.

Alumina-supported oxide precursors to Co_3Mo_3N/Al_2O_3 catalysts with theoretical loadings of 11, 15, 17.5, 20, 22.5, 28.5, and 35 wt % Co_3Mo_3N were prepared by impregnation of γ-Al_2O_3 with aqueous solutions of $Co(NO_3)_2 \cdot 6H_2O$ and $(NH_4)_6Mo_7O_{24} \cdot 4H_2O$ followed by calcination in air. The alumina was calcined at 773 K for 3 h in air prior to the first impregnation. The impregnated samples were dried overnight at 373 K after each successive impregnation. For example, the precursor to the 28.5 wt % Co_3Mo_3N/Al_2O_3 catalyst was prepared by impregnation of γ-Al_2O_3 (10.0 g) with an aqueous solution of $(NH_4)_6Mo_7O_{24} \cdot 4H_2O$, resulting in 4.40 g of $(NH_4)_6Mo_7O_{24}$ on the support after drying, with subsequent impregnation with an aqueous solution of $Co(NO_3)_2 \cdot 6H_2O$ to give 7.26 g of $Co(NO_3)_2$ on the support after drying. The impregnated alumina was calcined at 773 K for 3 h and then nitrided according to the following procedure. Approximately 1.0 g of the oxide precursor was degassed for 1 h at 295 K in 60 sccm He. Following degassing, the sample was heated from 295 to 1023 K at a rate of 2 K/min in 60 sccm NH_3. The Co_3Mo_3N/Al_2O_3 catalyst was furnace-cooled to room temperature in flowing ammonia and then passivated in a 60 sccm flow of 1 mol % O_2/He for 3 h prior to air exposure.

Synthesis of Co_3Mo_3C and Co_3Mo_3C/Al_2O_3. Co_3Mo_3N was prepared according to the procedure described above. Following furnace cooling in flowing ammonia (60 sccm), the intermediate product Co_3Mo_3N was degassed for 30 min in 60 sccm He at 295 K. Under continued He flow (60 sccm), the sample was heated to 673 K over 10 min, the flow switched to 60 sccm of a 20 mol % CH_4/H_2 mixture (Airgas), and the sample temperature increased from 673 to 950 K at a rate of 0.5 K/min. The flow was then switched to 60 sccm He and the Co_3Mo_3C product was furnace-cooled to room temperature. The bimetallic carbide was passivated in a 60 sccm flow of 1 mol % O_2/He for 3 h at room temperature prior to air exposure. In a related series of syntheses, the nitridation and passivation steps were kept the same, but the maximum TPR temperature achieved during the carburization step was increased incrementally from 298 to 950 K.

The following procedure was used to prepare Co_3Mo_3C/Al_2O_3 catalysts with theoretical loadings of 15, 20, and 22.5 wt % Co_3Mo_3C. Alumina-supported Co_3Mo_3N precursors with appropriate loadings were prepared as described above and then carburized according to the procedure described above for unsupported Co_3Mo_3C. Following synthesis, the Co_3Mo_3C/Al_2O_3 catalysts were passivated in a 60 sccm flow of 1 mol % O_2/He for 3 h at room temperature prior to air exposure. A series of syntheses were also carried out in which a 22.5 wt % Co_3Mo_3N/Al_2O_3 precursor was prepared as described above, but the maximum TPR temperature achieved in the carburization step was increased incrementally from 750 to 950 K.

Catalyst Characterization. *X-ray Diffraction Measurements.* X-ray diffraction (XRD) patterns were acquired on a Rigaku Geigerflex powder diffractometer using the Vaseline smear method. The system uses Cu Kα radiation ($\lambda = 1.5418$ Å) and is interfaced to a personal computer for data acquisition and analysis.

Transmission Electron Microscopy Measurements. Transmission electron microscope (TEM) images were acquired using a JEOL 2010 high-resolution transmission electron microscope operating at 200 keV. Samples of the alumina-supported bimetallic carbide and nitride catalysts as well as their oxide precursors were placed on a 200-mesh copper grid coated with Formvar and carbon.

Elemental Analysis. Metals analyses of bulk and alumina-supported bimetallic carbide and nitride catalysts were carried out by Huffman Laboratories, Inc. using inductively coupled plasma−atomic emission spectroscopy (ICP-AES). Carbon, hydrogen, and nitrogen (CHN) analyses of samples of Co_3Mo_3N and Co_3Mo_3C as well as of samples of intermediate composition, $Co_3Mo_3N_xC_y$, were carried out by Oneida Research Services, Inc. CHN analyses of the remaining catalysts were carried out by Huffman Laboratories, Inc.

(23) Yuhong, W.; Wei, L.; Minghui, Z.; Naijia, G.; Keyi, T. *Appl. Catal. A* **2001**, *215*, 39.

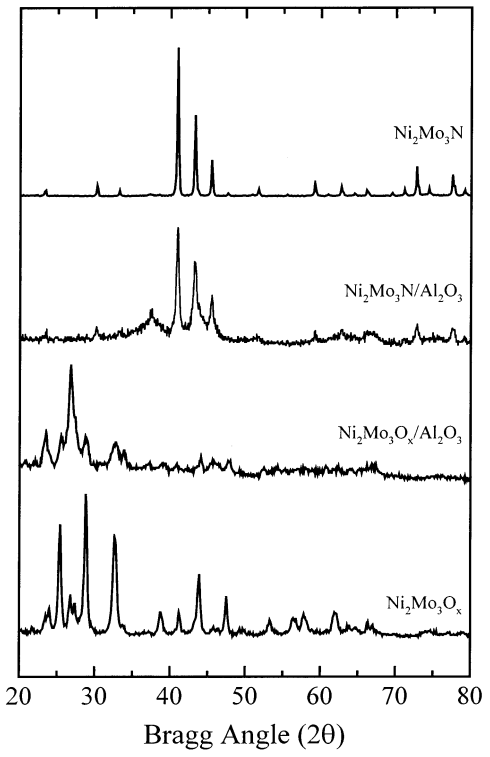

Figure 1. X-ray diffraction patterns for $Ni_2Mo_3O_x$, $Ni_2Mo_3O_x/Al_2O_3$, Ni_2Mo_3N/Al_2O_3, and Ni_2Mo_3N. The theoretical loading of the supported oxide precursor and bimetallic nitride is 50 wt % Ni_2Mo_3N.

BET and Pulsed Chemisorption Measurements. Single-point BET surface area measurements were obtained using a Micromeritics PulseChemisorb 2700 apparatus. Catalyst samples (~0.10 g) were placed in a quartz U-tube, degassed in a 60 sccm flow of He for 30 min at room temperature, followed by a 2-h degassing in a 45 sccm flow of He at 623 K and then cooled to room temperature under flowing He. A 35 sccm flow of a 28.65 mol % N_2/He mixture (Airco) was maintained during the surface area measurement. The instrument was calibrated with pure N_2 gas prior to a BET measurement. The He (Airgas, 99.999%) used was purified prior to use by passing it through 5A molecular sieve (Alltech) and O_2 (Oxyclear) purification traps.

Low-temperature O_2 pulsed chemisorption measurements were also carried out using the Micromeritics PulseChemisorb 2700 instrument. Chemisorption capacity measurements were conducted using a 10.3 mol % O_2/He mixture (Airco) as the probe gas. All catalyst samples (~0.10 g) were degassed in a 60 sccm flow of He at room temperature for 30 min and were then reduced prior to the chemisorption measurement. Samples were reduced by heating from room temperature to 673 K (6.3 K/min) in a 60 sccm flow of H_2 and holding at 673 K for 2 h. Finally, the samples were degassed in 45 sccm He at 673 K for 1 h.

Chemisorption capacities were measured by injecting a calibrated volume (0.101 mL) of the probe gas mixture at 1-min intervals into a constant flow of He (15 sccm) until O_2 uptake ceased. Prior to injection, the probe gas mixture was passed through a 1/8 in. coil of stainless steel tubing submerged in a pentane slush (~142 K). The O_2 chemisorption measurements were carried out with the catalyst samples held at 196 K.

Results

Ni_2Mo_3N and Ni_2Mo_3N/Al_2O_3. As shown in Figures 1 and 2, we have successfully prepared unsupported Ni_2Mo_3N as well as a series of Ni_2Mo_3N/Al_2O_3 catalysts (10−50 wt % Ni_2Mo_3N) by nitridation of unsupported and alumina-supported $Ni_2Mo_3O_x$ precursors, respectively, in flowing NH_3. The XRD pattern for the unsupported $Ni_2Mo_3O_x$ precursor (Figure 1) indicates that the material is a mixture of α-$NiMoO_4$ (card no. 33-0948)[24] and MoO_3 (card no. 35-0609),[24] which is consistent with the XRD pattern described by Alconchel et al.[25] On the other hand, the XRD pattern for a high-loading $Ni_2Mo_3O_x/Al_2O_3$ precursor (Figure 1) indicates that the supported phase consists primarily of β-$NiMoO_4$ (card no. 12-0348)[24] and MoO_3 (card no. 35-0609).[24] The XRD pattern for the material produced by nitridation of the unsupported precursor, shown in Figure 1, is identical to those reported by Alconchel et al.[25] and Herle et al.[26] for pure Ni_2Mo_3N. The elemental composition of the unsupported Ni_2Mo_3N, listed in Table 1, is consistent with that expected of the phase pure material.

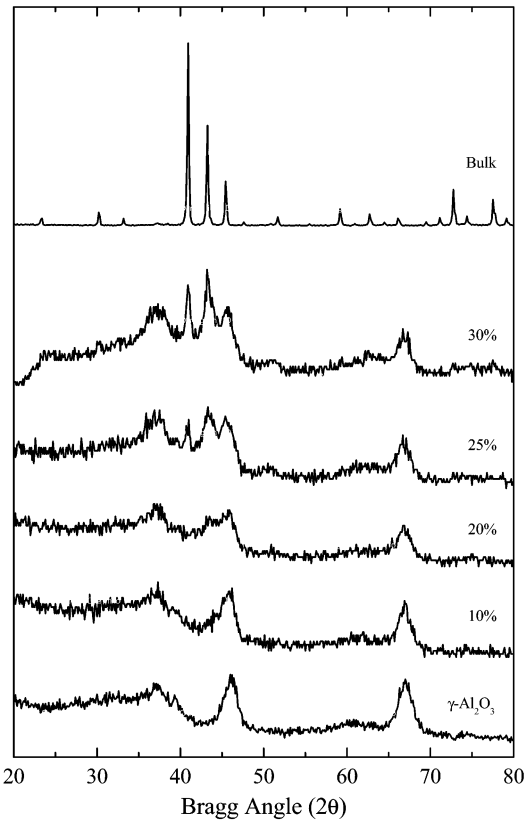

Figure 2. X-ray diffraction patterns for Ni_2Mo_3N/Al_2O_3 catalysts with theoretical loadings of 10, 20, 25, and 30 wt % Ni_2Mo_3N. Also shown for comparison purposes are the XRD patterns for γ-Al_2O_3 and Ni_2Mo_3N.

The XRD pattern for the Ni_2Mo_3N/Al_2O_3 catalyst in Figure 1 shows the same peaks as those of unsupported Ni_2Mo_3N as well as broad peaks located at ~37.5° and 67.0°, which are associated with the γ-Al_2O_3 support (card no. 47-1308).[24] The peak at ~37.5° may also indicate the presence of a small amount of γ-Mo_2N impurity (card no. 25-1366)[24] in the supported bimetallic nitride phase. The XRD patterns for a series of Ni_2Mo_3N/Al_2O_3 catalysts, shown in Figure 2, indicate that alumina-supported Ni_2Mo_3N can be prepared with a range of

(24) *JCPDS Powder Diffraction File*; International Centre for Diffraction Data: Swarthmore, PA, 2000.

(25) Alconchel, S.; Sapiña, F.; Beltrán, D.; Beltrán, A. *J. Mater. Chem.* **1999**, *9*, 749.

(26) Herle, P. S.; Hegde, M. S.; Sooryanarayana, K.; Row, T. N. G.; Subbanna, G. N. *Inorg. Chem.* **1998**, *37*, 4128.

Table 1. Elemental Composition of Bulk and Supported Bimetallic Catalysts

catalyst	composition (wt %)
Ni_2Mo_3N	calcd.: Ni 28.11, Mo 68.66, N 3.34 actual: Ni 27.98, Mo 68.59, N 3.43
Ni_2Mo_3N/Al_2O_3	calcd.: Ni 8.43, Mo 20.60, N 1.03 actual: Ni 7.84, Mo 18.36, N 2.07, C 0.06
Co_3Mo_3N	calcd.: Co 36.94, Mo 60.14, N 2.93 actual: Co 36.90, Mo 60.31, N 2.76, C 0.03
Co_3Mo_3N/Al_2O_3	calcd.: Co 8.31, Mo 13.53, N 0.66 actual: Co 7.97, Mo 12.96, N 1.68, C 0.04
Co_3Mo_3C	calcd.: Co 37.09, Mo 60.39, C 2.52 actual: Co 36.68, Mo 60.67, C 2.49, N 0.10
Co_3Mo_3C/Al_2O_3	calcd.: Co 8.31, Mo 13.53, C 0.66 actual: Co 7.82, Mo 12.69, C 0.35, N 0.19

crystallite sizes. For the 30 wt % Ni_2Mo_3N/Al_2O_3 catalyst, an average crystallite size of 16 nm can be calculated using the Scherrer equation and the full-width at half-maximum (fwhm) of the peak at 40.9°.[27] This crystallite size is considerably smaller than that reported by Jacobsen[28] of 44 nm for unsupported Ni_2Mo_3N. No XRD peaks associated with Ni_2Mo_3N are apparent above the background noise for loadings below 20 wt % Ni_2Mo_3N. The presence of Ni_2Mo_3N on the alumina support is inferred for the lower loadings, with the assumption that the crystallite size is below the detection limit for XRD.

Shown in Figure 3 are TEM micrographs of a 30 wt % Ni_2Mo_3N/Al_2O_3 catalyst, while elemental compositional information for this same catalyst is listed in Table 1. Inspection of Figure 3a indicates a range of Ni_2Mo_3N particle sizes, but no evidence for a crystalline impurity. Figure 3b shows an oval-shaped Ni_2Mo_3N particle on the alumina support having dimensions of 15 × 21 nm. The TEM micrograph in Figure 3b as well as others (not shown) yield *d*-spacing values of 2.11 and 2.80 Å for the {310} and {211} crystallographic planes of Ni_2Mo_3N, respectively, which are in good agreement with those from a simulated XRD pattern for Ni_2Mo_3N. The elemental composition of the supported Ni_2Mo_3N is compared with the theoretically calculated values in Table 1. The Ni and Mo loadings are slightly lower than the calculated values, while the N content is substantially higher. As discussed later, the high N content is likely due to the presence of nitrogen-containing species on the alumina support or adsorbed N species on the supported bimetallic nitride particles.

Listed in Table 2 are the BET surface area and O_2 chemisorption capacity for a Ni_2Mo_3N/Al_2O_3 catalyst with a 20 wt % Ni_2Mo_3N loading. The BET surface area of a 20 wt % Ni_2Mo_3N/Al_2O_3 catalyst is significantly higher than the value of 7 m^2/g reported by Jacobsen[28] for unsupported Ni_2Mo_3N. The chemisorption capacity of the reduced Ni_2Mo_3N/Al_2O_3 catalyst compares favorably with those measured previously for 10−20 wt % Mo_2N/Al_2O_3 catalysts, which were in the range 80−130 μmol/g.[6]

Co_3Mo_3N and Co_3Mo_3N/Al_2O_3. Shown in Figure 4 are XRD patterns for unsupported and alumina-supported oxide precursors as well as Co_3Mo_3N and Co_3Mo_3N/Al_2O_3 catalysts. The XRD pattern for the unsupported oxide precursor is in good agreement with

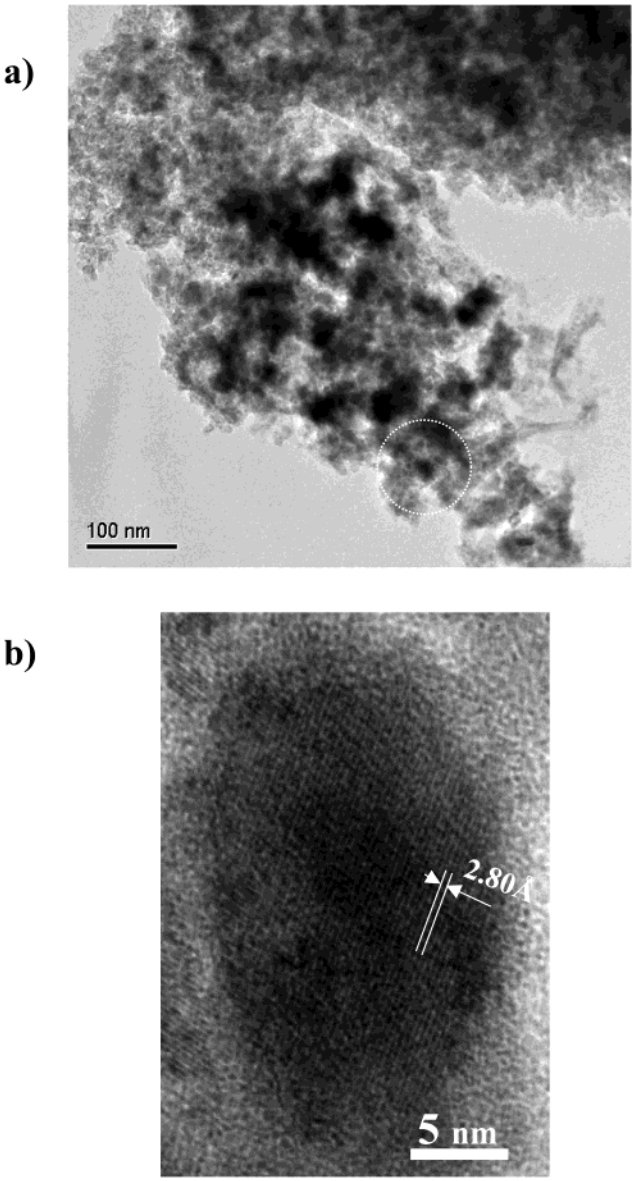

Figure 3. TEM micrographs of a 30 wt % Ni_2Mo_3N/Al_2O_3 catalyst.

Table 2. BET Surface Areas and Chemisorption Capacities for Catalysts with 20 wt % Nitride/Carbide Loadings

catalyst	surface area (m^2/g)	O_2 chemisorption capacity (μmol/g)
Ni_2Mo_3N/Al_2O_3	118	85.5
Co_3Mo_3N/Al_2O_3	111	114
Co_3Mo_3C/Al_2O_3	111	111

a reference pattern for β-$CoMoO_4$ (card no. 21-868), and the pattern for the supported oxide precursor shows the same peaks as well as those for the γ-Al_2O_3 support. After nitridation, the XRD pattern for the unsupported material (Figure 4) is in good agreement with published patterns for Co_3Mo_3N.[29,30] The elemental composition of the unsupported Co_3Mo_3N, listed in Table 1, is consistent with that expected of the phase pure material. Returning to Figure 1, the Co_3Mo_3N/Al_2O_3 catalyst,

(27) Suryanarayana, C.; Norton, M. G. *X-ray Diffraction*: *A Practical Approach*; Plenum Press: New York, 1998.
(28) Jacobsen, C. J. H. *Chem. Commun.* **2000**, 1057.
(29) Houmes, J. D.; Bem, D. S.; zur Loye, H.-C. *Mater. Res. Symp. Proc.* **1994**, *327*, 153.
(30) Alconchel, S.; Sapiña, F.; Beltrán, D.; Beltrán, A. *J. Mater. Chem.* **1998**, *8*, 1901.

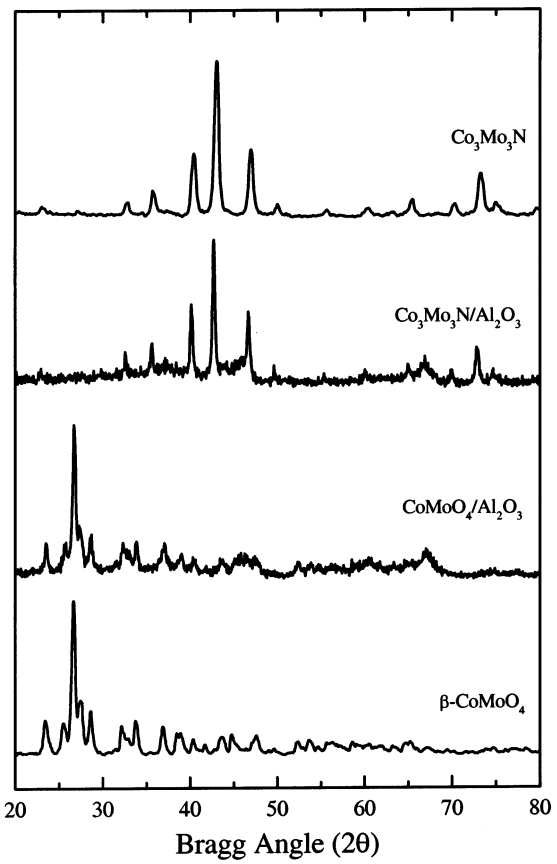

Figure 4. X-ray diffraction patterns for $CoMoO_4$, $CoMoO_4/Al_2O_3$,Co_3Mo_3N/Al_2O_3, and Co_3Mo_3N. The theoretical loading of the supported oxide precursor and bimetallic nitride is 35 wt % Co_3Mo_3N.

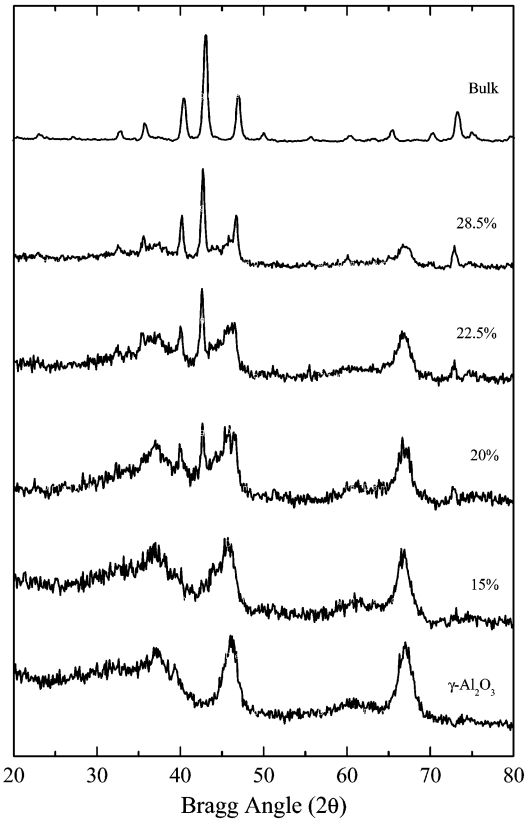

Figure 5. X-ray diffraction patterns for Co_3Mo_3N/Al_2O_3 catalysts with theoretical loadings of 15, 20, 22.5, and 28.5 wt % Co_3Mo_3N. Also shown for comparison purposes are the XRD patterns for γ-Al_2O_3 and Co_3Mo_3N.

which has a theoretical Co_3Mo_3N loading of 35 wt %, exhibits the same peaks as those observed for unsupported Co_3Mo_3N, confirming the presence of Co_3Mo_3N on the alumina support.

Shown in Figure 5 are the XRD patterns for a series of Co_3Mo_3N/Al_2O_3 catalysts with loadings in the range 15−28.5 wt % Co_3Mo_3N. A gradual increase in intensity of the peaks associated with Co_3Mo_3N is observed as the loading of the bimetallic nitride increases above 15 wt %. From the XRD pattern for the 22.5 wt % Co_3Mo_3N/Al_2O_3 catalyst, an average crystallite size of 21 nm is calculated for the supported Co_3Mo_3N particles using the Scherrer equation and the fwhm for the peak located at 42.7°. This crystallite size is smaller than the value of 36.3 nm reported by Hada et al.[31] for unsupported Co_3Mo_3N. TEM micrographs and elemental compositional information for the 22.5 wt % Co_3Mo_3N/Al_2O_3 catalyst can be found in Figure 6 and Table 1, respectively. Inspection of Figure 6a shows a fairly uniform dispersion of Co_3Mo_3N particles on the support with no evidence for a crystalline impurity. Figure 6b shows a high-resolution micrograph of a Co_3Mo_3N particle with an approximate diameter of 22 nm. This micrograph as well as others (not shown) yield *d*-spacing values of 2.22 and 6.25 Å for the {422} and {111} crystallographic planes of Co_3Mo_3N, respectively, which are in good agreement with those from a simulated XRD pattern for Co_3Mo_3N. The elemental composition of the supported Co_3Mo_3N is compared with the theoretically calculated values in Table 1. The Co and Mo loadings are slightly lower than the calculated values, while the N content is substantially higher. As for the Ni_2Mo_3N/Al_2O_3 catalyst, the high N content is likely due to the presence of N-containing species on the alumina support or adsorbed onto the bimetallic nitride particles that will be discussed later.

As given in Table 2, the 20 wt % Co_3Mo_3N/Al_2O_3 catalyst had a BET surface area of 111 m^2/g and an O_2 chemisorption capacity of 114 μmol/g. This surface area is considerably higher than the value measured by Hada et al.[31] of 12 m^2/g for unsupported Co_3Mo_3N. The O_2 chemisorption capacity value for the 20 wt % Co_3Mo_3N/Al_2O_3 catalyst can be compared to a value of 42.3 μmol/g reported previously from this laboratory for a 15 wt % Co_3Mo_3N/Al_2O_3 catalyst which contained either a Co−N or Co metal impurity.[19] The substantially higher chemisorption capacity measured for the Co_3Mo_3N/Al_2O_3 catalyst prepared in this study is likely due to the higher metal loading, to improved dispersion of the nitride phase, and possibly to the absence of the Co impurity phase. The chemisorption capacity for the Co_3Mo_3N/Al_2O_3 catalyst compares well with those for 15−20 wt % Mo_2N/Al_2O_3 catalysts that were discussed briefly above.

Co_3Mo_3C and Co_3Mo_3C/Al_2O_3. Unsupported Co_3Mo_3C was prepared via a two-step synthesis process in which β-$CoMoO_4$ was first nitrided to give Co_3Mo_3N and subsequently carburized to give Co_3Mo_3C. The XRD patterns for unsupported Co_3Mo_3N and Co_3Mo_3C are shown in Figure 7 along with a simulated XRD pattern

(31) Hada, K.; Nagai, M.; Omi, S. *J. Phys. Chem. B* **2001**, *105*, 4084.

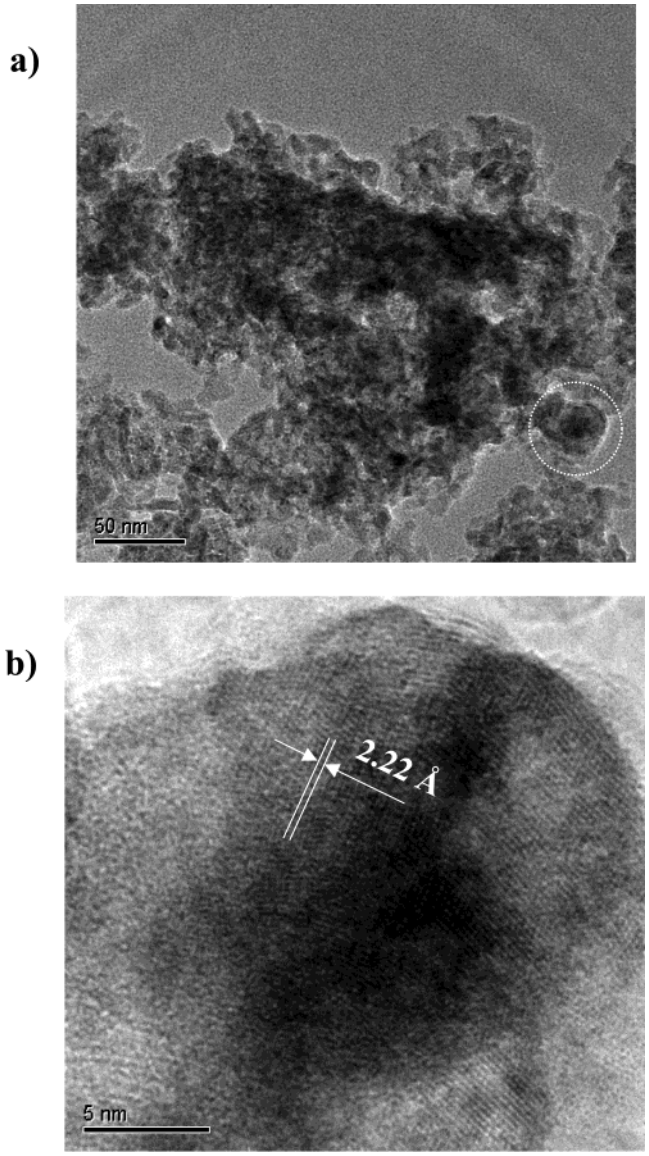

Figure 6. TEM micrographs of a 22.5 wt % Co_3Mo_3N/Al_2O_3 catalyst.

for Co_3Mo_3C. The simulated XRD pattern was calculated using PowderCell[32] as well as atomic coordinates and lattice parameters for Co_3Mo_3C published by Newsam et al.[33] based upon a Reitveld analysis of a neutron diffraction pattern for pure Co_3Mo_3C. The XRD patterns of Co_3Mo_3N and Co_3Mo_3C are nearly identical, reflecting the fact that the two materials have the same space group ($Fd3m$) and similar cubic cell parameters (Co_3Mo_3N, a = 11.02396(8) Å;[30] Co_3Mo_3C, a = 11.0709(3) Å[33]). However, close examination of the XRD patterns in Figure 7 reveals a small shift of the peaks for Co_3Mo_3C relative to those for Co_3Mo_3N, as indicated for the most intense peak in the two patterns. Elemental analysis of a sample of unsupported Co_3Mo_3C yielded metals and nitrogen contents that are in excellent agreement with the theoretically predicted values (see Table 1), providing additional evidence that the material is phase pure.

(32) Kraus, W.; Nolze, G. *J. Appl. Crystallogr.* **1996**, *29*, 3.
(33) Newsam, J. M.; Jacobson, A. J.; McCandlish, L. E.; Polizzotti, R. S. *J. Solid State Chem.* **1988**, *75*, 296.

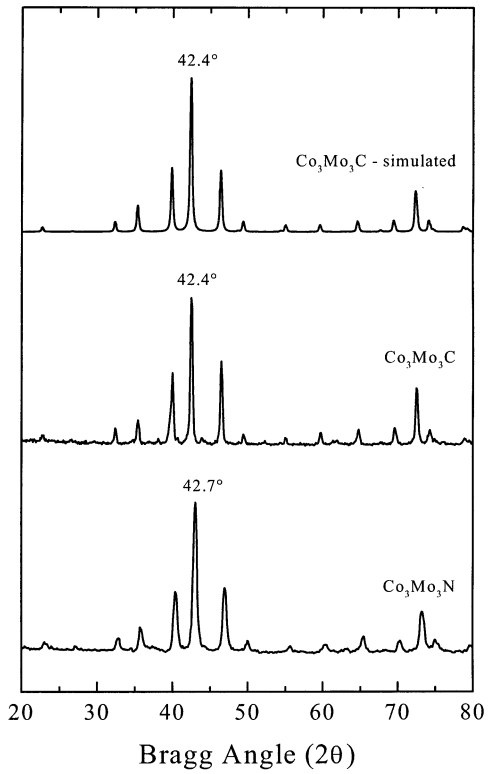

Figure 7. X-ray diffraction patterns for as-prepared Co_3Mo_3N and Co_3Mo_3C as well as a simulated XRD pattern for Co_3Mo_3C.

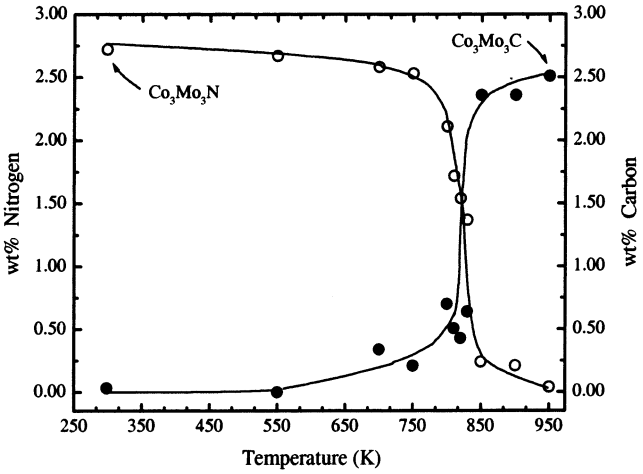

Figure 8. Weight percentage of nitrogen and carbon in $Co_3Mo_3N_xC_y$ products as a function of the maximum TPR temperature used for carburization of Co_3Mo_3N intermediates in 20 mol % CH_4/H_2.

Shown in Figure 8 are the nitrogen and carbon contents of a series of bimetallic Co−Mo materials, with variable compositions denoted as $Co_3Mo_3N_xC_y$, plotted as a function of the maximum temperature achieved during the carburization of unsupported Co_3Mo_3N. Significant replacement of nitrogen with carbon takes place for carburization temperatures above 750 K and is complete by 950 K. With these results in mind, samples of a 22.5 wt % Co_3Mo_3N/Al_2O_3 precursor were carburized to increasing temperatures in the range 750−950 K. The XRD patterns for these materials are shown in Figure 9. As indicated on the XRD patterns, the most intense peak gradually shifts from the value associated with alumina-supported Co_3Mo_3N (sample carburized at 750 K) to the value expected for alumina-

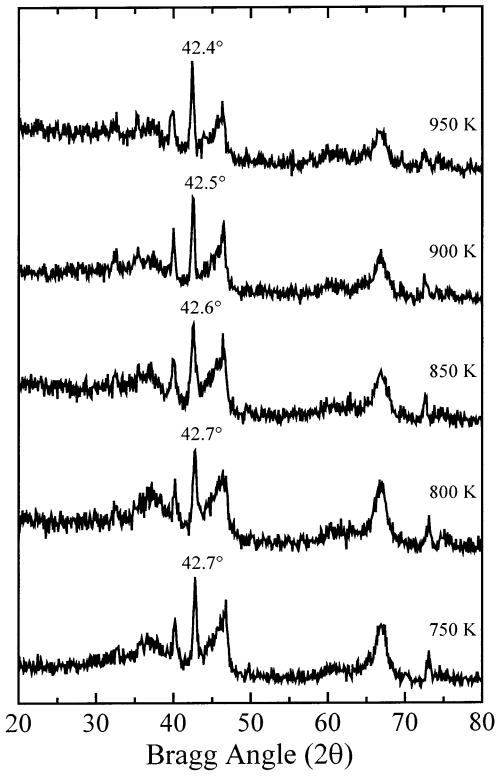

Figure 9. X-ray diffraction patterns for $Co_3Mo_3N_xC_y/Al_2O_3$ catalysts (22.5 wt % $Co_3Mo_3N_xC_y$) as a function of the maximum TPR temperature used for carburization of Co_3Mo_3N/Al_2O_3 intermediates (22.5 wt % Co_3Mo_3N) in 20 mol % CH_4/H_2.

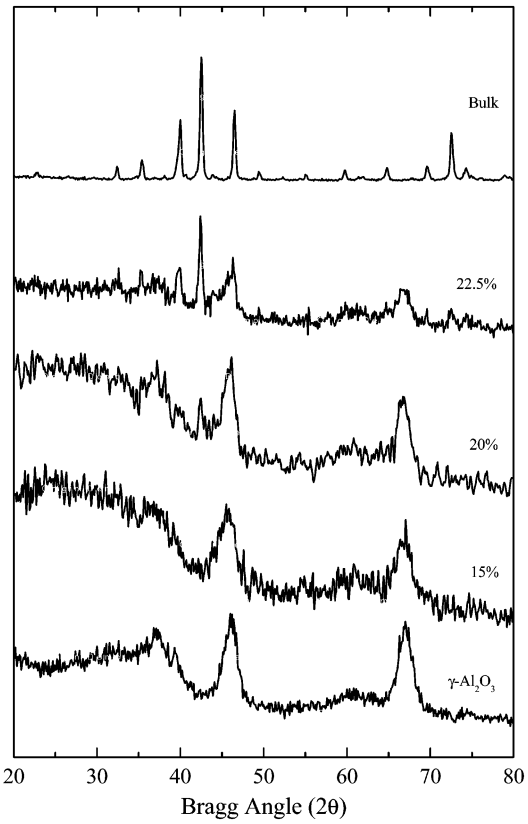

Figure 10. X-ray diffraction patterns for Co_3Mo_3C/Al_2O_3 catalysts with theoretical loadings of 15, 20, and 22.5 wt % Co_3Mo_3N. Also shown for comparison purposes are the XRD patterns for γ-Al_2O_3 and Co_3Mo_3C.

supported Co_3Mo_3C (sample carburized at 950 K). Co_3Mo_3C/Al_2O_3 catalysts with a range of loadings were prepared and XRD patterns for these catalysts are shown in Figure 10. From the XRD pattern for the 22.5 wt % Co_3Mo_3C/Al_2O_3 catalyst, an average crystallite size of 24 nm is calculated for the supported Co_3Mo_3C particles using the Scherrer equation and the fwhm for the peak located at 42.4°. Shown in Figure 11 are TEM micrographs for a 22.5 wt % Co_3Mo_3C/Al_2O_3 catalyst. The particle sizes apparent in Figure 11a are consistent with the average crystallite size measured by XRD. Figure 11b shows a high-resolution micrograph of a portion of a Co_3Mo_3C particle approximately 25 nm in length. Examination of this image as well as others (not shown) reveal *d*-spacing values of 3.88 and 6.35 Å for the {220} and {111} crystallographic planes of Co_3Mo_3C, respectively, which are in good agreement with those from the simulated XRD pattern for Co_3Mo_3C (see Figure 7). The elemental composition of the 22.5 wt % Co_3Mo_3C/Al_2O_3 catalyst is listed in Table 1. The metals and carbon contents are below the theoretically predicted values, and a significant nitrogen content was detected. On the basis of the elemental analysis, it is not possible to determine whether N is present in the bimetallic phase or on the support. As discussed later, the low carbon content (and the detected N) may indicate that there was incomplete replacement of nitrogen in the alumina-supported Co_3Mo_3N during the synthesis of the Co_3Mo_3C/Al_2O_3 catalyst.

The BET surface area of a 20 wt % Co_3Mo_3C/Al_2O_3 catalyst, 111 m^2/g, is identical to that of its Co_3Mo_3N/Al_2O_3 precursor and is substantially higher than the value reported by Xiao et al.[16] of 15.5 m^2/g for impure $Co_{0.5}Mo_{0.5}C_x$ prepared by direct carburization of a $CoMoO_4$ precursor. An O_2 chemisorption capacity of 111 μmol/g was measured for the 20 wt % Co_3Mo_3C/Al_2O_3 catalyst, which is slightly less than the value of 114 μmol/g measured for its Co_3Mo_3N/Al_2O_3 precursor. The O_2 chemisorption value for the 20 wt % Co_3Mo_3C/Al_2O_3 catalyst compares favorably with those measured previously for 10−20 wt % Mo_2C/Al_2O_3 catalysts that were in the range 100−130 μmol/g.[6]

Discussion

As noted in the Introduction, a number of studies have been published in which the catalytic properties of monometallic and bimetallic carbides and nitrides have been explored. These materials have drawn particular interest as potential catalysts for use in hydroteating processes such as hydrodesulfurization, where regulations requiring lower sulfur levels in transportation fuels are spurring the development of new catalysts. However, a rigorous understanding of the catalytic properties of oxide-supported bimetallic carbides and nitrides has been hampered by the fact that the supported bimetallic phases used in published studies were impure. The goal of the current study, therefore, has been to prepare phase pure, alumina-supported Ni_2Mo_3N, Co_3Mo_3N, and Co_3Mo_3C catalysts whose catalytic properties will be investigated in subsequent studies.

The incorrect identification of Ni−Mo−N phases has been the source of some confusion in the recent literature. Bimetallic nitrides initially identified to be pure Ni_3Mo_3N[34,35] were later determined to be impure ma-

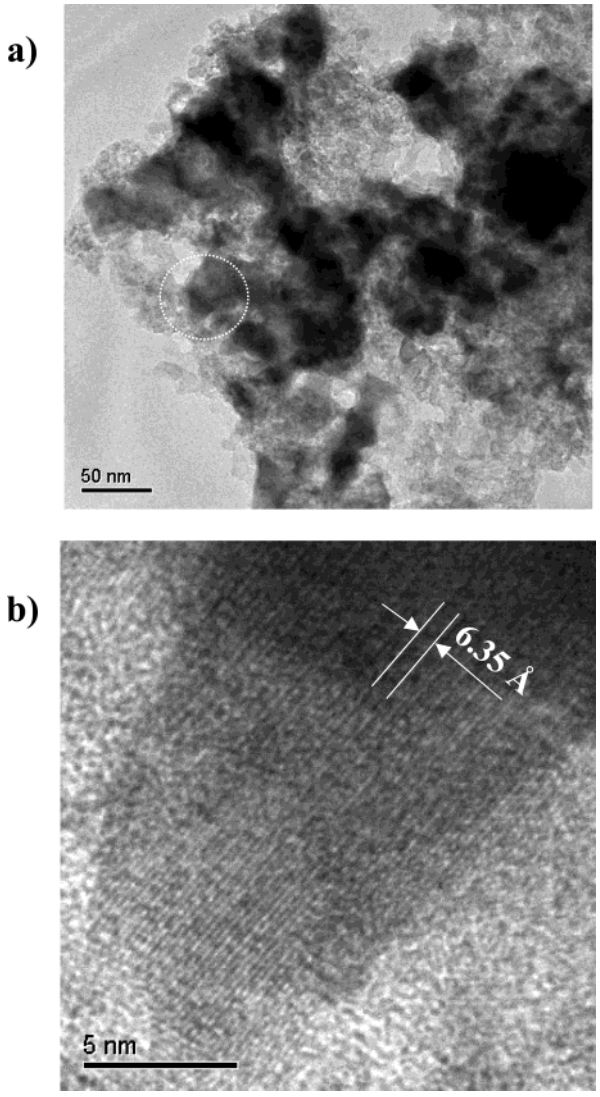

Figure 11. TEM micrographs of a 22.5 wt % Co_3Mo_3C/Al_2O_3 catalyst.

terials in which Ni_2Mo_3N was the major phase.[26,30] It was subsequently shown that pure Ni_2Mo_3N can be prepared by nitridation of metallorganic hydroxide[26] or bimetallic oxide[25,28] precursors in flowing NH_3. As described earlier, we have also successfully prepared Ni_2Mo_3N from a bimetallic oxide precursor. In contrast to the recent, successful reports of Ni_2Mo_3N synthesis, equally recent studies have been published describing the preparation of $Ni-Mo-N/Al_2O_3$ catalysts in which the major nitride phase was erroneously identified to be Ni_3Mo_3N.[20,23] In both cases, XRD patterns are reported for $Ni-Mo-N/Al_2O_3$ catalysts prepared from oxidic precursors with Ni/Mo = 1.0. In addition to "Ni_3Mo_3N", Chu et al.[20] note the presence of a substantial Ni impurity in their catalyst while the XRD pattern of the catalyst prepared by Yuhong et al.[23] shows a substantial γ-Mo_2N impurity. The syntheses differ in that Chu et al.[20] carried out their nitridation using NH_3 and a maximum TPR temperature of 973 K while Yuhong et al.[23] used a 10 mol % H_2/N_2 mixture and a maximum TPR temperature of 823 K.

To our knowledge, the synthesis of alumina-supported Ni_2Mo_3N reported in the current study is the first in which a pure, oxide-supported Ni−Mo−N phase has been prepared. The alumina-supported oxidic precursor had the appropriate metal stoichiometry (Ni/Mo = 0.67) and was nitrided in flowing NH_3 to a maximum TPR temperature of 1173 K. The results of Chu et al.,[20] Yuhong et al.,[23] and the current work are consistent with the thorough studies of Alconchel et al.[25,30] in which the synthesis conditions were varied systematically for oxidic precursors with Ni/Mo ratios of 0.67 and 1.0. Nitridation of a Ni/Mo = 1.0 precursor to a maximum TPR temperature of 873 K yielded a Ni−Mo−N material with substantial Mo−N (MoN, Mo_2N) and $Ni_{0.2}Mo_{0.8}N$ impurities while nitridation of this same oxidic precursor to 1073 K produced a Ni_2Mo_3N sample containing an unidentifiable Ni impurity. Nitridation of a Ni/Mo = 0.67 precursor to a maximum TPR temperature of 1223 K yielded the desired Ni_2Mo_3N product.

Evidence for the purity of the bimetallic phase in the Ni_2Mo_3N/Al_2O_3 catalysts prepared in the current study is based upon XRD and TEM measurements as well as elemental analyses. The XRD patterns of Ni_2Mo_3N/Al_2O_3 catalysts with loadings of 25 wt % and higher are in good agreement with those of pure Ni_2Mo_3N reported in this study and by others.[25,26] For loadings of 20 wt % and lower, it is assumed that the Ni_2Mo_3N crystallite size is below the XRD detection limit and, therefore, the presence of the bimetallic phase on the alumina support is inferred for these loadings. TEM micrographs and metals analysis of a 22.5 wt % Ni_2Mo_3N/Al_2O_3 catalyst are consistent with the identification of phase pure Ni_2Mo_3N on the alumina support, while the N content is not. The high N content, 2.07 wt % compared to the expected value of 1.03 wt %, is most likely due to the presence of N-containing species on the uncovered alumina areas of the catalyst or adsorbed to the surfaces of the bimetallic nitride particles. High N contents have been reported for Mo_2N/Al_2O_3 catalysts prepared using conditions similar to those employed in the synthesis of the Ni_2Mo_3N/Al_2O_3 catalysts.[36−38] Dolce et al.[36] measured N/Mo ratios = 0.75−1.26, compared to an expected value of N/Mo = 0.5, for Mo_2N/Al_2O_3 catalysts with a range of loadings that were prepared via NH_3 TPR in conditions similar to those utilized in the current study. Dolce et al.[36] attributed the high N contents of their catalysts to N-containing species on the support; a sample of γ-Al_2O_3 nitrided under the same conditions used to prepare the Mo_2N/Al_2O_3 catalysts had an N content of 0.4 wt %. This level of nitrogen on the alumina is insufficient to account for the discrepancy of the calculated and expected N contents of the highest loading Mo_2N/Al_2O_3 catalyst prepared by Dolce et al.[36] or the 22.5 wt % Ni_2Mo_3N/Al_2O_3 catalyst prepared in this study. It is conceivable that spillover of N-containing species from the metal-containing phases to the support may significantly increase the N content of the alumina. Nitrogen-containing species adsorbed on the surfaces of the metal nitride particles may also be responsible for the high N content of the catalyst.

(34) Bem, D. S.; Gibson, C. P.; zur Loye, H.-C. *Chem. Mater.* **1993**, *5*, 397.
(35) Weil, K. S.; Kumta, P. N. *Mater. Sci. Eng. B* **1996**, *38*, 109.
(36) Dolce, G. M.; Savage, P. E.; Thompson, L. T. *Energy Fuels* **1997**, *11*, 668.
(37) Yang, S.; Li, C.; Xu, J.; Xin, Q. *J. Phys. Chem. B* **1998**, *102*, 6986.
(38) Hada, K.; Nagai, M.; Omi, S. *J. Phys. Chem. B* **2000**, *104*, 2090.

While adsorbed N species would not be expected to contribute substantially to the N content of a low surface area, unsupported bimetallic nitride, this may be important for well-dispersed, oxide-supported nitride particles.

The synthesis of unsupported Co_3Mo_3N was first reported by Houmes et al.[29] Alconchel et al.[30] studied the synthesis of Co_3Mo_3N in some detail and determined that the purity of the material is dependent on the maximum temperature achieved during the TPR synthesis in flowing NH_3. For maximum temperatures below 1073 K, the authors observed substantial amounts of an unidentified impurity having XRD peaks in the range 40−45°. Alconchel et al.[30] prepared phase pure Co_3Mo_3N via a TPR synthesis with a maximum temperature of 1173 K and a 50 sccm NH_3 flow. In the current study, we have prepared Co_3Mo_3N using a slightly modified TPR synthesis employing a lower maximum temperature (1023 K) and a higher NH_3 flow (100 sccm).

A number of laboratories have reported the synthesis of nitrided $Co-Mo/Al_2O_3$ catalysts,[17,19,22,39] but in only one case was XRD used to identify the bimetallic phase. Logan et al.[19] described a synthesis for the preparation of Co_3Mo_3N/Al_2O_3 catalysts, but the supported Co_3Mo_3N contained a significant Co−N or Co metal impurity as indicated by an XRD peak at 44.5°. The TPR synthesis of this catalyst utilized a maximum temperature of 970 K and a 60 sccm flow of NH_3, followed by cooling of the catalyst from 970 K to room temperature in flowing He (30 sccm). In the current study, Co_3Mo_3N/Al_2O_3 catalysts with a range of loadings have been prepared, none of which have an XRD peak at 44.5°, suggesting that the supported Co_3Mo_3N is free of the crystalline impurity detected in the earlier synthesis. On the basis of the XRD data alone, it is not possible to exclude the presence of this impurity phase in the form of crystallites that are too small to detect by XRD. Consistent with the XRD results, there is no evidence of impurity phases in TEM micrographs of a 22.5 wt % Co_3Mo_3N/Al_2O_3 catalyst. The synthesis procedure described in the current study differs from that reported by Logan et al.[19] in two respects: the maximum TPR temperature reached was 1023 K, and the catalysts were furnace-cooled in flowing NH_3. Similar to the results for the 30 wt % Ni_2Mo_3N/Al_2O_3 catalyst discussed earlier, elemental analysis of a 22.5 wt % Co_3Mo_3N/Al_2O_3 catalyst revealed slightly lower metal contents than the theoretically predicted values, but also a substantially higher than expected N content. As for the Ni_2Mo_3N/Al_2O_3 catalyst, we believe the high N content can be traced to N-containing species on the uncovered alumina areas of the catalyst or to N-containing species adsorbed on the surfaces of the Co_3Mo_3N particles.

Excluding syntheses that involve arc-melting of the elements, relatively few studies have been published that describe the synthesis of unsupported Co_3Mo_3C. Newsam et al.[33] described a method for preparing Co_3Mo_3C that involves two primary steps: (1) heating cobalt trisethylenediamine molybdate ($Co(en)_3MoO_4$; en = $H_2NCH_2CH_2NH_2$) in an H_2/He mixture over the temperature range 298−923 K to give an unknown intermediate precursor, followed by (2) heating the precursor to 1273 K in a CO/CO_2 mixture. The high temperature needed to convert the intermediate precursor to the bimetallic carbide makes this synthesis unattractive for the preparation of high surface area Co_3Mo_3C in either an unsupported or a supported form. More recently, Green and co-workers[16] reported the TPR synthesis of a series of Co−Mo carbides prepared by carburization of oxidic precursors with Co/Mo ratios in the range 0.25−1.0. The authors used 10 vol % C_2H_6/H_2 as the carburization gas mixture and the maximum temperature achieved during the TPR synthesis was 900 K. For an oxidic precursor with Co/Mo = 1, carburization yielded an impure product principally composed of β-Mo_2C and Co metal. For lower Co/Mo ratios, the authors conclude that the carburized materials, while impure, contain substantial amounts of Co_3Mo_3C as determined by XRD.[16]

Consistent with the results of Green and co-workers,[16] attempts in our laboratory to prepare unsupported and alumina-supported Co_3Mo_3C via carburization of oxidic precursors were unsuccessful. The products in all cases were impure materials, whether unsupported or supported, which consisted primarily of β-Mo_2C and Co metal. The two-step synthesis procedure described in the current study for the preparation of unsupported and supported Co_3Mo_3C was adapted from a synthesis first reported by Volpe and Boudart[40] for the preparation of α-MoC_{1-x} ($x \approx 0.5$) from γ-Mo_2N. This conversion is a topotactic process, with the product carbide retaining the structure of the starting material, γ-Mo_2N. Green and co-workers[4] have recently reported that a similar two-step synthesis procedure can be used to prepare bimetallic carbide materials such as $W_9Nb_8C_x$ and $Mo_3Nb_2C_x$. In their study, the authors also include a lucid discussion of what constitutes a pseudomorphic or topotactic reaction. Our observation that Co_3Mo_3C can be prepared from Co_3Mo_3N is not surprising, given the similar structures and lattice parameters for the two materials. As described by Alconchel et al.,[30] Co_3Mo_3N is an interstitial nitride (like γ-Mo_2N) in which N atoms reside only in interstices defined by Mo atoms. One might expect, therefore, that the N atoms in Co_3Mo_3N could be replaced in a topotactic process with C atoms to give Co_3Mo_3C. While we do not present sufficient data in this study to confirm the topotactic nature of the synthesis of Co_3Mo_3C from Co_3Mo_3N, it seems likely that this is such a reaction.

To our knowledge, no reports have appeared in the literature describing the synthesis of Co_3Mo_3C in oxide-supported form. Consistent with the synthesis of unsupported Co_3Mo_3C, replacement of N in a 22.5 wt % Co_3Mo_3N/Al_2O_3 catalyst with C can be accomplished via TPR in a flowing 20 mol % CH_4/H_2 mixture to a maximum temperature of 950 K. The XRD pattern of the resulting 22.5 wt % Co_3Mo_3C/Al_2O_3 catalyst shows the identical shift of the XRD peak positions from their values for the corresponding nitride as observed for unsupported Co_3Mo_3N. The *d* spacings measured from TEM micrographs of the 22.5 wt % Co_3Mo_3C/Al_2O_3 catalyst are also consistent with successful synthesis of Co_3Mo_3C on the support. The elemental analysis, how-

(39) Yang, S.; Li, Y.; Xu, J.; Li, C.; Xin, Q.; Rodriguez-Ramos, I.; Guerrero-Ruiz, A. *Phys. Chem. Chem. Phys.* **2000**, *2*, 3313.

(40) Volpe, L.; Boudart, M. *J. Solid State Chem.* **1985**, *59*, 332.

ever, suggests that the replacement of N with C is not complete. Assuming that the nitrogen and carbon contents measured in the elemental analysis are associated only with the bimetallic phase, a formula of $Co_{3.00}Mo_{3.00}C_{0.66}N_{0.31}$ is calculated. Other explanations include the possibility that the nitrogen is associated with the alumina support and that the low C content is due to incomplete combustion of the carbon in the oxide-supported Co_3Mo_3C. The measured carbon content, while below the theoretically predicted value, does indicate that excess carbon has not been deposited on the catalyst surface. The deposition of excess carbon (amorphous or graphitic) on the catalyst surface is a drawback of the TPR synthesis method that has been noted in a number of studies in which the preparation of unsupported β-Mo_2C and Mo_2C/Al_2O_3 catalysts has been investigated.[7,41,42]

The composition of the bimetallic phase of the 22.5 wt % Co_3Mo_3C/Al_2O_3 catalyst suggests additional work may be necessary to determine the optimal synthesis conditions for achieving full replacement of N in the supported catalyst. In preparing Mo_2C/Al_2O_3 catalysts via carburization of Mo_2N/Al_2O_3 precursors, Oyama and co-workers[7] encountered difficulty in attaining complete replacement of N with C. A Mo_2N/Al_2O_3 catalyst carburized in a flowing 20 mol % CH_4/H_2 mixture to a maximum TPR temperature of 973 K yielded a supported phase of composition $Mo_2N_{0.66}C_{0.73}$ instead of the desired Mo_2C. These authors found that increasing the maximum temperature achieved during the TPR synthesis to 1173 K resulted in additional (but still incomplete) N replacement, but also resulted in the deposition of substantial amounts of excess carbon on the catalyst surface.

One final point that should be addressed is the dispersion of the alumina-supported Ni_2Mo_3N, Co_3Mo_3N, and Co_3Mo_3C. As discussed earlier, monometallic and bimetallic carbides and nitrides have drawn interest as potential catalysts for a number of processes. To fully exploit this potential, it is necessary to optimize the dispersion of the bimetallic phase. X-ray diffraction and TEM images indicate that significantly smaller particle sizes can be achieved (relative to published values for the unsupported materials[16,28,31]) by supporting Ni_2Mo_3N, Co_3Mo_3N, and Co_3Mo_3C on γ-Al_2O_3. Furthermore, the oxygen chemisorption measurements reveal that the catalysts have high adsorption site densities, similar to those reported in the literature for Mo_2N/Al_2O_3 and Mo_2C/Al_2O_3 catalysts.[6]

Conclusion

Synthesis procedures have been developed for the preparation of alumina-supported Ni_2Mo_3N, Co_3Mo_3N, and Co_3Mo_3C catalysts having high surface areas and O_2 chemisorption capacities. Studies are in progress in which the hydrotreating properties of these materials are being investigated, with particular focus on their catalytic activities and sensitivity to pretreatment conditions, as well as their resistance to deep sulfidation under hydrotreating reaction conditions.

Acknowledgment. This research was supported by the National Science Foundation under Grant CHE-9610438. Acknowledgment is also made to the Henry Dreyfus Teacher-Scholar Awards Program of the Camille and Henry Dreyfus Foundation for partial support of this research. A portion of the research (TEM) described in this paper was performed in the Environmental Molecular Sciences Laboratory, a national scientific user facility sponsored by the Departments of Energy's Office of Biological and Environmental Research and located at Pacific Northwest National Laboratory. The authors would like to acknowledge Drs. C. H. F. Peden and C. Wang for helpful discussions and Stephanie J. Sawhill for carrying out the BET and chemisorption measurements.

CM011508J

(41) Lee, J. S.; Lee, K. H.; Lee, J. Y. *J. Phys. Chem.* **1992**, *96*, 362.
(42) Hanif, A.; Xiao, T.; York, A. P. E.; Sloan, J.; Green, M. L. H. *Chem. Mater.* **2002**, *14*, 1009.